

## STACKED MICROSTRIP PATCH ANTENNAS

J.R. MOSIG, L. BARLATEY and F.E. GARDIOL  
Ecole Polytechnique Fédérale, EL-Ecublens, CH-1015 Lausanne, Switzerland

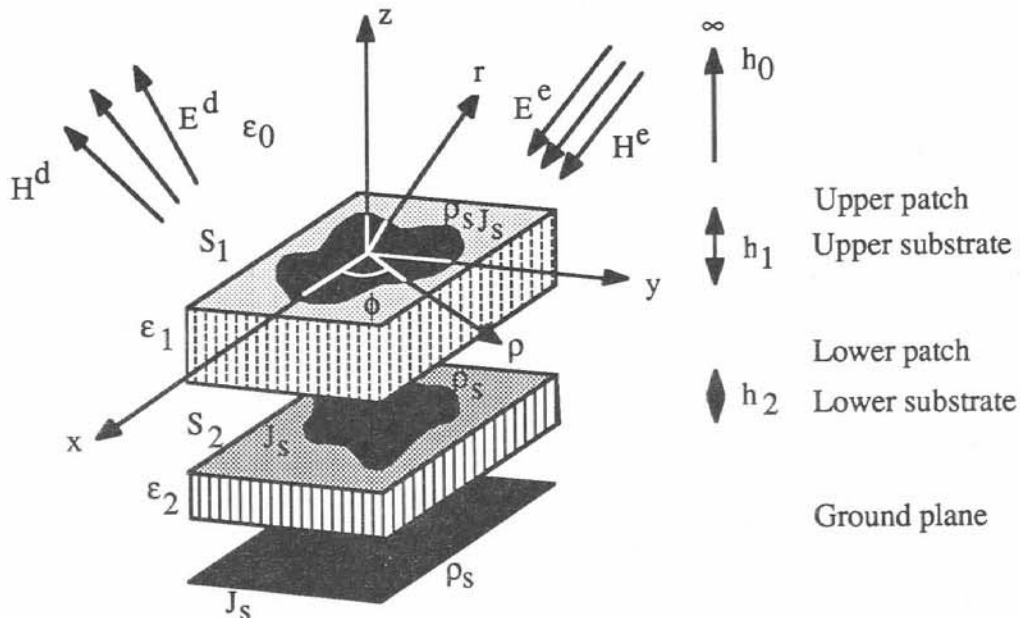
### 1. INTRODUCTION

The use of several dielectric layers yields additional degrees of freedom to improve the performance of microstrip antenna bandwidth, beamwidth, gain and efficiency [1]. A simple configuration is a patch covered by a thin protective radome [2]. The cover layer may also be ice or dust, that adversely affect the performance. A two-layer geometry was considered to study electromagnetically coupled dipoles [3] and a proximity coupled patch [4]. Future monolithic integrated arrays will mostly use a multilayered technology. Active devices may be integrated on a lower substrate layer, and connected to antennas above. The active devices require high permittivity substrates, whereas a low permittivity enhances the antenna's efficiency [5].

By stacking two patches in a double-layer substrate, the antenna's bandwidth can be increased, up to 10%, while gains larger than 10 dB have been reported [6]. Dual frequency operation is also possible with patches of different sizes [7].

The analysis of stacked patches presents a rather complex problem in electromagnetics, where simple approaches like the cavity model fail. It can be handled with the more rigorous integral equation approach. A full-wave treatment of stacked microstrip antennas in a double-layer substrate was developed, using a mixed potential integral equation in the space domain combined with a method of moments.

### 2. INTEGRAL EQUATION



The structure considered, shown in **figure 1**, includes two dielectric layers with stacked patches  $S_1$  and  $S_2$ . An integral equation for the surface currents  $J_S$  on both patches is deduced from the continuity of the tangential electric field on a conducting object .

$$\vec{e}_z \times [\vec{E}^e + \vec{E}^d] = Z_S \vec{e}_z \times \vec{J}_S \tag{1}$$

where  $\vec{E}^e$  is the excitation (impressed) field and  $\vec{E}^d$  is the diffracted (induced) field, produced by the surface currents. Conductor losses are accounted for by the surface impedance  $Z_S$ , ratio of the tangential electric field by the surface current density. The upper conductor thickness is generally negligible when compared to the substrate, so that the radiating conductors can be modeled by electric current sheets, and the surface impedance given by  $Z_S = (1 + j) \sqrt{\pi f \mu_0 / \sigma}$ .

The diffracted electric field is derived from a scalar potential  $V$  and a vector potential  $\vec{A}$ , expressed in terms of Green's functions that only exhibit weak singularities. The problem can thus be solved in the space domain, where the physical interpretation is easier, and where simple approximations can be obtained in the near and far fields. This approach was previously developed for a single layer microstrip patch [8]. In terms of the Green's functions for the potentials  $\vec{G}_A$  and  $G_V$ , acting respectively on the surface current density  $\vec{J}_S$  and on the surface charge density  $\rho_S$ , the boundary condition (1) becomes

$$\vec{e}_z \times \vec{E}^e(\vec{r}) = \vec{e}_z \times \left[ Z_S \vec{J}_S(\vec{r}) + j\omega \int_{S'} dS' \vec{G}_A(\vec{r}/\vec{r}') \vec{J}_S(\vec{r}') + \nabla \int_{S'} G_V(\vec{r}/\vec{r}') \rho_S(\vec{r}') dS' \right] \quad (2)$$

This is the mixed potential integral equation (MPIE), applied on the surface of both patches  $S = S_1 \cup S_2$ . No magnetic currents are assumed to flow on the patches. This MPIE is a Fredholm integral of the second kind, but since the term  $Z_S \vec{J}_S$  is usually quite small, it behaves numerically as a Fredholm integral of the first kind. The dyadic Green's function  $\vec{G}_A$  is given by (there are no vertical currents, hence no need to consider the  $zz$  - component):

$$\vec{G}_A = \left( \vec{e}_x G_A^{xx} \vec{e}_x + \vec{e}_z G_A^{zx} \vec{e}_x \right) + \left( \vec{e}_y G_A^{yy} \vec{e}_y + \vec{e}_z G_A^{zy} \vec{e}_y \right) + \vec{e}_z G_A^{zz} \vec{e}_z \quad (3)$$

Where  $G_A^{xx}$  and  $G_A^{zx}$  are the components of the vector potential created by an  $x$ -directed horizontal electric dipole. The scalars  $G_A^{yy}$  and  $G_A^{zy}$  are obtained by a change of coordinates.

The microstrip structure is assumed to be infinite in the transverse directions, so that the Green's functions exhibit a translational invariance along  $x$  and  $y$ . The Green's function  $G_V$  associated with the scalar potential is defined by :

$$\nabla_t \cdot \vec{G}_A = \mu \epsilon \nabla G_V \quad (4)$$

In free space,  $\vec{G}_A = \vec{U} \mu_0 \Psi$  with  $\Psi = \exp(-jk_0 r) / 4\pi r$  where  $\vec{U}$  is the unit dyadic, and then  $G_V = \Psi / \epsilon_0$ . The situation gets more involved in stratified media [8]

### 3. NUMERICAL ALGORITHMS

The integral equation is solved with a method of moments, using identical basis and test functions (Galerkin). Our calculations consider rectangular patches, on which the entire domain basis functions are the eigenmodes associated with the patches. On more complicated geometries, subsectional basis functions such as those employed for the single layer case [8] can be introduced. Let  $\vec{J}_S$  be the surface current density on the patch at the interface between layers  $i-1$  and  $i$ :

$$\vec{J}_{S_i} = \sum_{k=1}^{N_i} \alpha_{k,i} \vec{f}_{k,i} \quad (i = 1, 2) \quad \text{with} \quad \vec{f}_{k,i} = \vec{e}_x \sin\left(\frac{m_x \pi x}{a_i}\right) \cos\left(\frac{n_x \pi y}{b_i}\right) + \vec{e}_y \cos\left(\frac{m_y \pi x}{a_i}\right) \sin\left(\frac{n_y \pi y}{b_i}\right) \quad (5)$$

where  $a_i, b_i$  are the dimensions of the  $i$ -th. patch and the integers  $m_x, n_x, m_y, n_y$  refer to the eigenmode considered and are functions of the indexes  $k$  and  $i$ . In general, if we select  $N_i$  non zero modes to expand the unknown  $\vec{J}_S$ , the total number of unknowns in the method of moments will be  $N = N_1 + N_2$ . Associated with the current there is a surface charge given by the continuity equation as :

$$\rho_{S_i} = \sum_{k=1}^{N_i} \alpha_{k,i} h_{k,i} \quad \text{with} \quad h_{k,i} = -\nabla_t \cdot \vec{f}_{k,i} / j\omega \quad (6)$$

The excitation considered here is a coaxial probe attached to the lower patch and modelled by a zero thickness filament of current  $I$ . Consequently, according to continuity equation, the excitation charge is a point charge  $+I / j\omega$  located at the probe's insertion point. The application of the method of moments then proceeds along well known steps, and finally the integral equation reduces to a matrix equation  $C\vec{\alpha} = \vec{b}$  which is solved for the unknown amplitudes  $a_{k1}$  and  $a_{k2}$ . In general the matrix  $C$  contains elements of the form :

$$c_{ki,lj} = j\omega \int_{S_i} dS_i \int_{S_j} dS'_j \vec{f}_{ki} \cdot \overline{\overline{G_A}} \vec{f}_{lj} + \int_{S_i} dS_i \int_{S_j} dS'_j h_{ki} G_V h_{lj} + Z_S \int_{S_i} dS_i \vec{f}_{ki} \cdot \vec{f}_{lj} \quad (7)$$

and the excitation terms are of the form :

$$b_{lj} = \int_{S_j} G_V h_{lj} dS_j \quad (8)$$

A succesful numerical analysis must include an efficient and accurate technique to evaluate the Green's functions, expressed by Sommerfeld integrals over a semi-infinite interval (Hankel transforms), for which specific algorithms were developed. For the single layer case, they were given in a previous publication [8]. The integrands become more involved in the double layer case, but the numerical techniques developed previously are still useful. Even with pre-computed Green's functions stored in interpolating tables, the numerical evaluation of the matrix is very cumbersome due to four-fold integrals. Fortunately, the change of variables

$$x - x' = p_1 \quad y - y' = q_1 \quad x + x' = p_2 \quad y + y' = q_2 \quad (11)$$

reduces the problem to a double spatial integration on  $p_1, q_1$ . Integrations over  $p_2$  and  $q_2$  are performed analytically. A transformation to polar coordinates removes the spatial singularity in the diagonal terms. This feature reduces considerably the CPU time and increases the integration's accuracy. Once the matrix equation has been solved and the amplitude coefficients  $a_{k1}, a_{k2}$  are known, the input impedance to the coaxial-fed stacked antenna is computed by evaluating the voltage at the insertion point [8].

#### 4. RESULTS

**Figure 2** depicts the first configuration analyzed and measured, designed to work as a dual frequency antenna. The substrate is composed of two identical layers with  $\epsilon_r = 2.33$ ,  $\tan \delta = 0.0012$  and  $h = 0.51$  mm.. The lower patch is 28 X 18 mm., fed by a coaxial probe centered along the  $y$ -coordinate and at 10 mm. from the edge. The upper patch has the same width (18 mm.) but is slightly longer (31.2 mm.) to provide dual frequency operation. The theoretical analysis is performed with one mode per patch. The theoretical predictions (dotted line) are compared to the experiment (solid line). The discrepancy between predicted and measured resonant frequencies is less than 1 % at the lower resonance and 4 % at the higher resonance. These errors may be due to the glue (cyanolit) between the two layers.

The second configuration (fig. 3), with two identical stacked square patches (8X8 mm.), provides broadband operation. The two layers are identical ( $\epsilon_{r1} = \epsilon_{r2} = 2.33$ ,  $\tan \delta_1 = \tan \delta_2 = 0.001$   $h_1 = h_2 = 1.57$  mm.). The lower patch is excited along its diagonal at 2.8 mm. from a corner. The upper patch is shifted 1 mm. in the x - direction (offset stacked patches). The theoretical results agree well with measurement over the range 8.5 - 11 GHz, showing the accuracy of the numerical technique. Here 2 modes per patch were used in the computation. After matching, the bandwidth for a VSWR less than 2 is expected to be greater than 15%, .

## 5. CONCLUSION

A rigorous technique is presented to analyze stacked microstrip patches in a two-layer environment. The mixed potential integral equation is solved with a method of moments and theoretical results for the input impedance of a two layer patch are in good agreement with measurements. The slight deviation between the curves is attributed to tolerance errors in the permittivity and the loss tangent as well as construction defects. While the resonant frequencies are primarily determined by the patch length , they are significantly affected by the coupling.

## REFERENCES

- [1] H.K. Smith, and P.E. Mayes, "Stacking resonators to increase the bandwidth of low profile antennas", IEEE Trans. Antennas and Propagation, vol. AP-35, no. 12, pp. 1473-1476, Dec. 1987
- [2] N.G. Alexopoulos and D.R. Jackson, "Fundamental superstrate (cover) effects on printed circuit antennas", IEEE Trans. Antennas and Propagation, vol AP-32, no 8, pp. 807-808, 1984
- [3] A.J.M. Soares, S.B.A. Fonseca and A.J. Giarola, "The effects of a dielectric cover on the current distribution and input impedance of printed dipoles", IEEE Trans. on Antennas Propagation, vol. AP-32, no. 11, pp. 1149-1153, Nov. 1984
- [4] D.M. Pozar and B. Kaufmann, "Increasing the bandwidth of a microstrip antenna by proximity coupling", Electronics Letters, vol. 23, pp. 368-369, April 9 , 1987
- [5] P.B. Katehi and N.G. Alexopoulos, "A bandwidth enhancement method for microstrip antennas", IEEE Trans. on Antennas and Propagation, vol. AP-35, no.1, pp..5-12., January 1987.
- [6] R.Q. Lee and K.F. Lee, "Gain enhancement of microstrip antennas with overlaying parasitic directors", Electronics Letters, vol.24, no.11, pp.656-658, May 26, 1988
- [7] S.A. Long and M.D. Walton, "A dual frequency stacked circular disc antenna", IEEE Trans. on Antennas and Propagation, vol. AP-27, no. 2, pp. 270-273, March 1979
- [8] J. Mosig, and F.E. Gardiol "General integral equation formulation for microstrip antennas and scatterers," Proc. IEE, pt. H, vol. 132, pp. 424-432, 1985

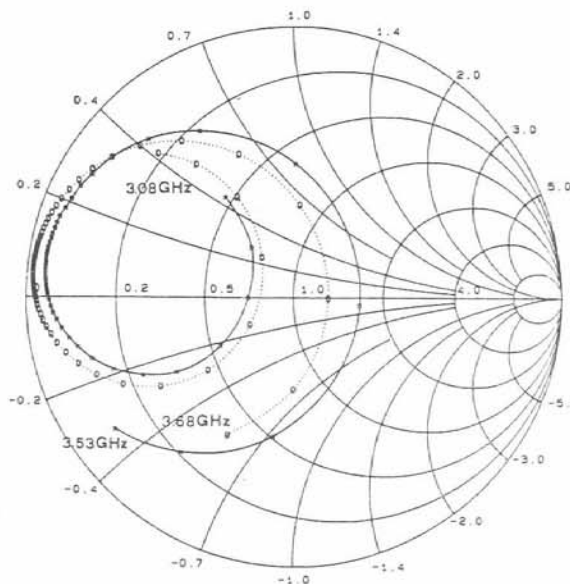


Fig. 2 : Input impedance of the dual frequency stacked antenna between 3.08 and 3.68 GHz (0.1 GHz frequency step)

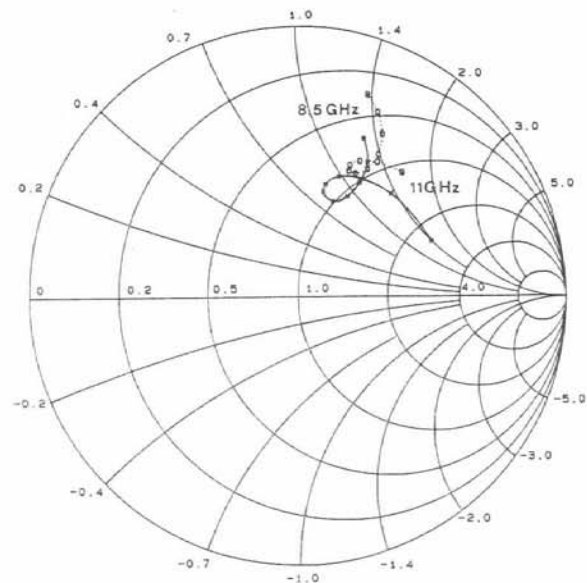


Fig. 3 : Input impedance of the broadband stacked antenna between 8.5 and 10 GHz (0.25 GHz frequency step)

Solid line : experimental data ; dotted line : experiment